Available online at www.sciencedirect.com

ScienceDirect

Procedia Structural Integrity 31 (2021) 134–139

Structural Integrity Procedia

www.elsevier.com/locate/procedia

4th International Conference on Structural Integrity and Durability, ICSID 2020

Layered model of crack growth in concrete beams in bending

I. Kožar[a,*], N. Bede[a], S. Mrakovčić[a], Ž. Božić[b]

[a] *University of Rijeka, Faculty of Civil Engineering, R. Matejčić 3, 51000 Rijeka, Croatia*
[b] *University of Zagreb, Faculty of Mech. Eng. And Nav. Arch., Zagreb, Croatia*

Abstract

Fracture properties of various types of concrete, like plain or fiber reinforced concrete are determined in 3-point bending experiments resulting in a force-displacement diagram. Standard properties of concrete are then determined using technical norms. However, post-peak behavior of concrete, including crack propagation, cannot be described using standard properties. Authors are developing nonlinear, stochastically based material model for concrete to describe post-peak concrete behavior together with crack propagation. One of the most desirable properties of the model is its suitability for later in-verse analysis and parameter determination. Model is based on moment – curvature (m-κ) relation and layered approach to discretization. In this work, we are presenting the basic properties of the model and its ability to capture the phenomena of interest (proof of concept).

Keywords: bending behavior; force-displacement; post-peak behavior; crack propagation; fracture; stochastically based model;

Nomenclature

f_c	force - displacement function for concrete defined in piecewise terms
ϵ	position of the neutral axis in beam's cross section
κ	curvature of the beam
h_i	position of i^{th} layer
m	moment acting in beam's cross section
F	force balance function
M	moment balance function

* Corresponding author. Tel.: +385 51 265-993.
E-mail address: ivica.kozar@gradri.uniri.hr

2452-3216
10.1016/j.prostr.2021.03.022

1. Introduction

Fracture behavior of concrete is mostly characterized with crack propagation, which becomes easily exposed under bending of concrete specimens. Three-point bending is standard experimental procedure for determination of relevant fracture properties of various types of concrete, like plain or fiber reinforced concrete. Specimens could be with or without a notch (as in our case, compare Beigrezaee et al. (2019)) and loading process could be considered quasi-static (see e.g., Gomez et a,. (2020)). Result of an experiment is obtained as the force – displacement diagram where the peak load determines the boundary of fracture behavior of concrete. Before the peak load, the specimen behavior is mostly linear or moderately nonlinear without visible large cracks; from that area in the diagram standard properties of concrete (modulus of elasticity, compressive strength, etc.) are determined using technical norms (e.g., see ASTMC 1609M (2012)). After the peak load the specimen is in the softening regime characterized with appearance of visible cracks and their rapid propagation, compare Čakmak et al. (2019) or Lukács (2019) or Majidi et al. (2019) or Arandjelović et al. (2020). The post-peak behavior, together with crack propagation cannot be described using standard material properties. Authors are developing nonlinear, stochastically based material model for concrete to describe post-peak concrete behavior together with the crack propagation Kožar et al. (2019) and Kožar et al. (2020). Authors' intention is to further develop the model and use it later for inverse analysis, parameter estimation and eventual damage assessment, see Kožar et al. (2018) and Pastorcic et al. (2019). Plans for later investigation include analysis of low cycle fatigue (similar to Cazin et al. (2020)] and based on Kožar and Ožbolt (2010)).

Model is based on an already known moment – curvature (m-κ) relationship (see e.g., Kišiček and Sorić (2003)), however, layered approach for cross-section discretization in a post-peak analysis is a novelty. Beam cross-section is divided into a number of layers where each layer obeys a force – displacement relation and force contributions from all the layers comprise force balance and moment balance equations. Behavior of each layer could be derived using various approaches (e.g., see Ferro and Berto (2020)) but here we assume it to be known.

Laboratory experiments have been performed where concrete beams with and without fibers were exposed to three point bending (see Bede and Mrakovčić (2020)). The resulting force – displacement diagrams have been used for evaluation of the numerical model. In this work we are presenting the basic properties of the model and its ability to capture the post-peak beam regime, i.e., we are presenting the proof of concept for a layered beam model.

2. Experimental analysis

Laboratory experiments have been performed consisting of three-point bending of high strength concrete beams with and without fibers. In this work, we are interested only in beams without fibers; they will set the reference for beams with fibers that would be analyzed later. Nine beams have been tested; dimensions were 100 x 100 x 400 mm with 300 mm span between the supports, without notch. The flexure tests were carried out by means of a servo-controlled hydraulic machine at the laboratory of the Faculty of Civil Engineering in Rijeka. The resulting load-displacement history was recorded up to the deflection of min 3 mm to obtain the post-peak behavior. The testing setup is presented in Fig. 1. It could be seen that beam without fibers (Fig. 1.(a)) is very brittle and it is not simple to properly record its full load – displacement diagram that includes the post-peak regime.

Fig. 1. Three-point bending tests for: (a)) beam without fibers; (b)) beam with fibers.

For beams without fibers, one is typically interested in displacement up to the peak load as is shown in Fig. 2.(a). Including the post-peak regime into the diagram full force-displacement behavior is recorded as shown in Fig. 2.(b). Fig. 2.(b) shows results for flexure of all the nine specimens and their mean that has been calculated (thick green line). The mean curve has been used as a reference for numerical analysis. It is interesting to observe how a sharp bi-linear load – displacement curves from individual flexure experiments trans-form into a well-known softening curve for the mean result.

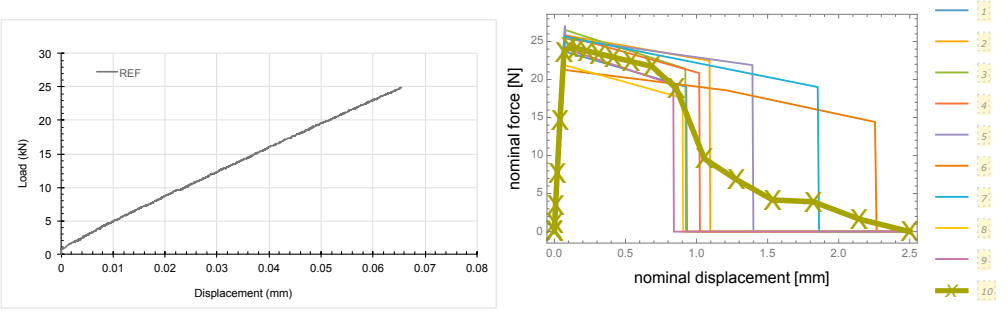

Fig. 2. Experimental results for beam without fibers: a) from testing machine up to the peak load; b) statistics after the peak load.

3. Numerical model

Numerical model is based on an already known moment – curvature (m-κ) relationship that has rather long tradition in engineering analysis of beams. This analysis is usually limited to the pre-peak load intensity level and the cross-section is not discretized, it is described with a relation, instead. In our work cross-section is discretized into layers where the number of layers determines accuracy and smoothness of the solution. Optimization of the number of layers is not in the focus of this work and it has been determined by experience, in our case 12. Each layer has equal force – displacement relation described with the equation

$$f_c(x,a,b_c,b_t) = \begin{cases} a\,x\,E\,exp\dfrac{-ax}{b_c} \;\; if \;\; x<0 \\ a\,x\,E\,exp\dfrac{-ax}{b_t} \;\; if \;\; x\geq 0 \end{cases} \tag{1}$$

where a and b are shape parameters (b_c for the compression part of material deformation and b_t for the tension part), E is modulus of elasticity. The material model determines formulation of the function; we have taken fiber bundle model to represent our material behavior (see e.g., Mishnaevsky (2011)); also, the function is similar to one in the microplane material model Ožbolt et al. (2001). Fig. 3.(a) presents the influence of parameters a and b on shape of the function and Fig. 3.(b) demonstrates different behavior of the function in tension and compression (since b_c and b_t are generally different). This different behavior of the function in different sections of domain requires a special solution procedure that takes into account that the function is in different domain for each layer. Our model is built in Wolfram Mathematica (2020) where the function is described as a 'piecewise' function so that even more complicated domain segmentation could be taken into account.

Bending model is based on two equilibrium equations, force balance

$$F(\epsilon,\kappa) = \Delta h \sum_{i=1}^{layers} f_c\left[(h_i-\epsilon h)\,tan(\kappa)\right] = 0 \tag{2}$$

and moment balance

$$M(\epsilon,\kappa) = \Delta h \sum_{i=1}^{layers} (h_i-\epsilon h)\cdot f_c\left[(h_i-\epsilon h)\,tan(\kappa)\right] = m \tag{3}$$

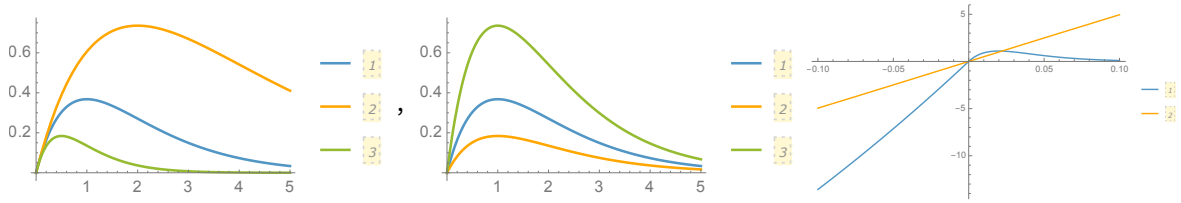

Fig. 3. Force-displacement law for each layer: a) influence of parameter a and b; b) whole force-displacement diagram for concrete (curved) and (eventual) reinforcement (straight).

where ϵ is the normalized neutral axis position and κ is the curvature, h is the cross-section height, h_i is position of layer i, Δh is height of each layer and $layer$ is total number of layers and f_c (force - displacement function for concrete) is given above.

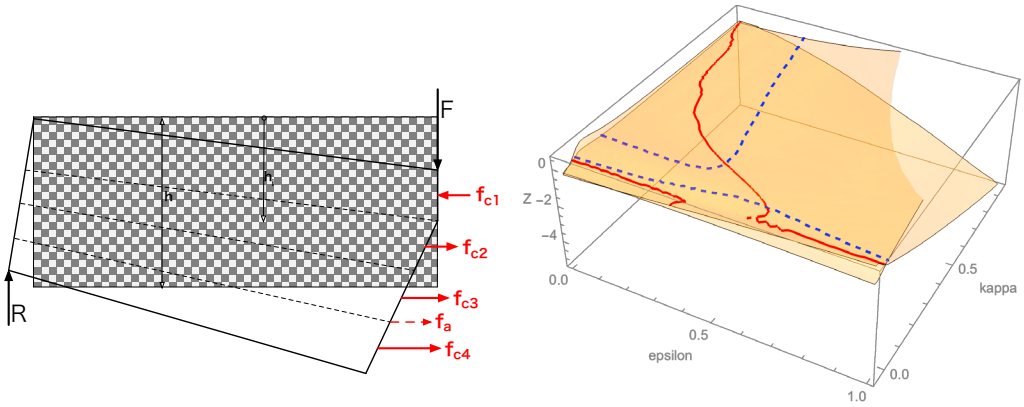

Fig. 4. Three-point bending models: a) geometry of layers; b) equilibrium equations (force-red, moment-blue).

Beam geometry relevant for equilibrium equations is given in Fig. 4.(a). Fig. 4.(b) is a graphical representation of the system of equilibrium equations. Red line stands for force equation and blue line stands for moment equation. It is visible that there are two solutions depicted as cross sections of the red and blue lines (it is there that both equations are satisfied). One solution corresponds to the pre-peak equilibrium and the other for the post-peak equilibrium. Existence of two solutions for one loading moment requires careful tracking of parameters ϵ and κ during the solution process. In this work, we have applied the 'arc-length' method. Table 1 gives an example of two solutions for moment $m = 0.1$.

Table 1. Equilibrium solutions for M=0.1.

parameter	1^{st} solution	2^{nd} solution
Neutral axis ϵ	0.43324	0.19938
Curvature κ	0.1547	0.7085

Fig. 5. presents forces in layers of the cross-section as the beam passes through the peak load, blue based colors are for compression and red based colors are for tension. Cross-section is discretized into 12 layers, 13^{th} been reserved for (optional) reinforcement that has not been activated in our analysis. In Fig. 5.(a) cross-section is in the pre-peak regime, in Fig. 5.(b) at the peak load and in Fig. 5.(c) in the post-peak regime. Note that the external loading (moment) is the same in Fig. 5.(a) and (c).

Fig. 6. presents full range of physically relevant solutions; Fig. 6.(a) shows normalized neutral axis position and Fig. 6.(b) moment – curvature relation. Shape of the two functions in Fig. 6. depends on the geometry of the specimen and parameters in the function f_c.

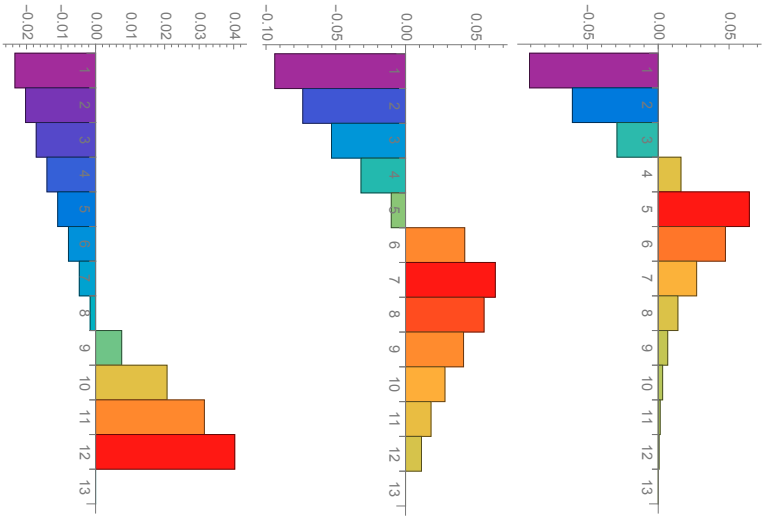

Fig. 5. Three-point bending cross-section forces for: a) m=0.05 (pre-peak); b) m=0.10 (peak); c) m=0.05 (post-peak).

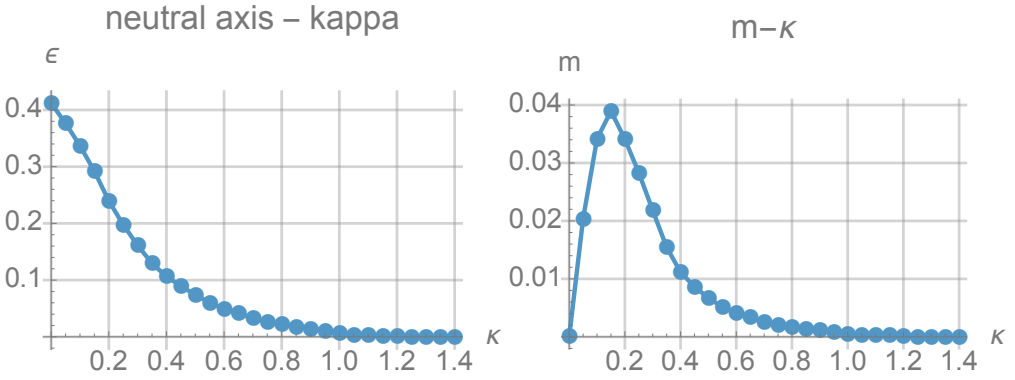

Fig. 6. Three-point bending model results for parameter $a = 5$ in function f_c: a) $\epsilon - \kappa$; b) $m - \kappa$ diagram.

4. Conclusion

In this work, we have presented experimental results for concrete beams under three-point bending. We have devised a model suitable for description of crack propagation during experiments. Model parameters have been determined only approximately as a proof of concept. Numerical results from the model successfully qualitatively describe experimental results. In future work we will apply procedures as in Kožar et al. (2019) and Kožar et al. (2018) to develop an inverse model of crack propagation in beams under bending. That should enable us to determine parameter values in the model up to a desired level of accuracy.

Acknowledgements

This work has been supported through project HRZZ 7926 ”Separation of parameter influence in engineering modeling and parameter identification” and project KK.01.1.1.04.0056 ”Structure integrity in energy and transportation”, which is gratefully acknowledged.

References

Beigrezaee, M.J., Ayatollahi, M.R., Bahrami, B., da Silva, L.F.M.,2019. Failure load analysis in single lap joints - effect of adherend notching. Engineering Failure Analysis 104, 75-83.

ASTMC1609/C1609M-12. 2012. Standard test method for flexural performance of fiber-reinforced concrete (using beam with third-point loading), ASTM Committee.

Čakmak, D., Tomičević, Z., Wolf, H., Božić, Ž., Semenski, D., Trapić, I., 2019. Vibration fatigue study of the helical spring in the base-excited inerter-based isolation system. Engineering Failure Analysis 104, 44-56.

Lukács, J., 2019. Fatigue crack propagation limit curves for high strength steels based on two-stage relationship. Engineering Failure Analysis 104, 431-442.

Majidi, H.R., Torabi, A.R., Zabihi, M., Razavi, S.M.J., Berto, F., 2019. Energy-based ductile failure predictions in cracked friction-stir welded joints. Engineering Failure Analysis 104, 327-337.

Kožar,I., Toric Malic, N., Smolcic, Ž., Simonetti, D., 2019. Bond-slip parameter estimation in fibre reinforced concrete at failure using inverse stochastic model. Engineering Failure Analysis 104, 84–95.

Kožar, I., Torić Malić, N., Simonetti, D., Božić, Ž., 2020. Stochastic properties of bond-slip parameters at fibre pull-out. Engineering Failure Analysis 111, 104478.

Kožar, I., Toric Malic, N., Rukavina, T., 2018. Inverse model for pullout determination of steel fibers. Coupled System Mechanics 7, 197–209.

Pastorcic, D., Vukelic, G., Bozic, Ž., 2019. Coil spring failure and fatigue analysis. Engineering Failure Analysis 104, 310-318.

Kišiček, T., Sorić, Z., 2003. Bending moment - curvature diagram for reinforced-concrete girders (in Croatian). Journal of Civil Engineering 55, 207–215.

Bede, N., Mrakovčić, S., 2020. Flexure behaviour of high strength concrete with steel and polypropilene fibres. In: 2nd International Conference on Construction Materials for Sustainable Future (in print), 15-17 April 2020, Bled, Slovenia.

Mishnaevsky, L., 2011. Hierarchical composites: Analysis of damage evolution based on fiber bundle model. Composites Sciences and Technology 71, 450-460.

Ožbolt, J., Yijun, L., Kožar, I., 2001. Microplane Model for Concrete with Related Kinematic Constraint. International journal of solids and structures, 38(16), 2683-2711.

Wolfram Research Inc., Mathematica, 2020. URL: https://www.wolfram.com/mathematica/.

Gomez, Q., Uenishi, K., Ionescu., I.R., 2020. Quasi-static versus dynamic stability associated with local damage models. Engineering Failure Analysis 111, 104476.

Cazin, D., Braut, S., Božić, Ž., Žigulić R., 2020. Low cycle fatigue life prediction of the demining tiller tool. Engineering Failure Analysis 111, 104457.

Arandjelović, M., Sedmak, S.A., Milović, Lj., Maksimović, A., Božić, Ž., 2020. Crack propagation in 3PB specimen made from welded joint. Procedia Structural Integrity 28, 440–445.

Ferro, P., Berto, F., 2020. The strain energy density approach applied to bonded joints. Procedia Structural Integrity 28, 19–25.

Kožar, I. and Ožbolt, J., 2010. Some aspects of load-rate sensitivity in visco-elastic microplane material model. Computers & Concrete 7, 331-346.